Angewandte Chemie
Eine Zeitschrift der Gesellschaft Deutscher Chemiker

Supporting Information

69451 Weinheim, Germany

Control over Rectification in Supramolecular Tunneling Junctions**

Kim S. Wimbush, William F. Reus, Wilfred G. van der Wiel, David N. Reinhoudt, George M. Whitesides, Christian A. Nijhuis, and Aldrik H. Velders**

anie_201003286_sm_miscellaneous_information.pdf

Experimental Details

Materials: Preparation of heptathioether-functionalized β-cyclodextrin[1] and G1-PPI-$(Ad)_4$,[2] G1-PPI-$(Fc)_4$[3] and G1-PPI-$(BFc)_4$[4] dendrimers was described previously. We characterized all compounds with Nuclear Magnetic Resonance Spectroscopy (^{1}H NMR) and Mass Spectrometry (MALDI ToF and ESI-MS), with all compounds yielding similar results to what has been previously published. Eutectic Gallium Indium was used as purchased from Aldrich.

Method:

SAM Formation

Ultra flat substrates of thin films of gold metal on a polymer supported by a glass slide, were obtained by delaminating an evaporated film of gold from a Si/SiO_2 template (the 'mechanical template-stripping' procedure (TS)) as previously described in detail.[5] βCD SAMs were prepared by immersing freshly cleaved ultra flat gold substrates into a 0.1-1mM solution of βCD dissolved in ethanol for 16hrs at 60°C. The substrates were removed and placed in a vial of fresh warm ethanol with the vial being gently agitated for one to two minutes. After removal they were further rinsed with ethanol (room temperature) and MilliQ water, and then dried under a stream of dry nitrogen. As previously published, Electrochemical Impedance Spectroscopy was used to characterize control βCD SAMs and yielded similar results.

Dendrimer Absorption

Substrates that were to contain dendrimers were immersed in an aqueous solution of the corresponding dendrimer-βCD assembly; G1-PPI-$(Ad)_4$ and G1-PPI-$(Fc)_4$ dendrimer, 2-3mM in Ad/Fc concentration in the presence of 2-3mM of βCD at pH = 2 for at least 1hr, G1-PPI-$(BFc)_4$ dendrimer, 1-2mM in BFc functionality in the presence of 10mM βCD at pH =2, for at least 2.5hrs.[4, 6] Subsequently the samples were rinsed with MilliQ water and dried under a stream of dry nitrogen. As previously published, Surface Plasmon Resonance and Cyclic Voltammetry were used to characterize the control βCD SAM + dendrimer assemblies and yielded similar results.

EGaIn Junction Formation and Electrical measurements

The EGaIn top contact 75.5 % Ga 24.5 % In by weight was formed by bifurcating a drop of EGaIn between a needle and a clean film of Au.[7] The resulting conical tip was carefully brought into contact with the surface of the molecular structure. A wire directly attached to the metal needle on the syringe connected the EGaIn electrode electrically with an electrometer (Keithley 6430). The supporting Au substrate served as the common (ground) electrode by means of a gold needle that penetrated the SAM and contacted the Au directly. A triaxial cable connected the two electrodes to an external amplifier. The electrometer applied a bias, *V*, across the junction. A positive value of *V* corresponded with EGaIn being biased positively with respect to the Au. The entire setup, except the source-meter was housed in a home-built aluminum Faraday cage. For each molecular junction structure (i-iv), current density (*J*) was measured as a function of voltage (*V*) across a minimum of 21 individual EGaIn junctions, formed over a minimum of 3 individual 1cm × 1cm Au^{TS} substrates (2-7 EGaIn junctions per substrate). For each EGaIn junction 20 scans were measured ± 2.0 V, with one scan consisting of a voltage sweep, 0.0 V → + 2.0 V → 0.0 V → - 2.0 V → 0.0 V.

Statistical Analysis

As mentioned in the paper, and as previously published,[8] an in depth statistical analysis was carried out for all molecular junctions. Each averaged $|J|$ vs. V scan was calculated by plotting the $|J|$ measured at each voltage value (step size 0.10 V, in both sweep directions) into histograms, giving in total 82 individual histograms corresponding to the number of times a particular value of $|J|$ was measured at that particular voltage. All histograms were plotted on a log scale, giving a normal distribution, allowing the data to be fit with Gaussian curves. This gave the average $|J|$ (the log mean) and the error (one-log standard deviation, 68% of the data is within one log standard deviation of the log-mean) for each voltage value, allowing the construction of the average $|J|$ vs. V scan, with one single data point on the graph representing one Gaussian fit histogram. Figure S1 gives an example on how the averaged data points were calculated**.** Figure S2 shows the individual semi log plots of the averaged (log mean) $|J|$ vs. V, for all EGaIn supramolecular junction structures. In each plot the error bars represent one log standard deviation from the log mean value, indicating between which J values 68% of our total obtained J measurements lie.

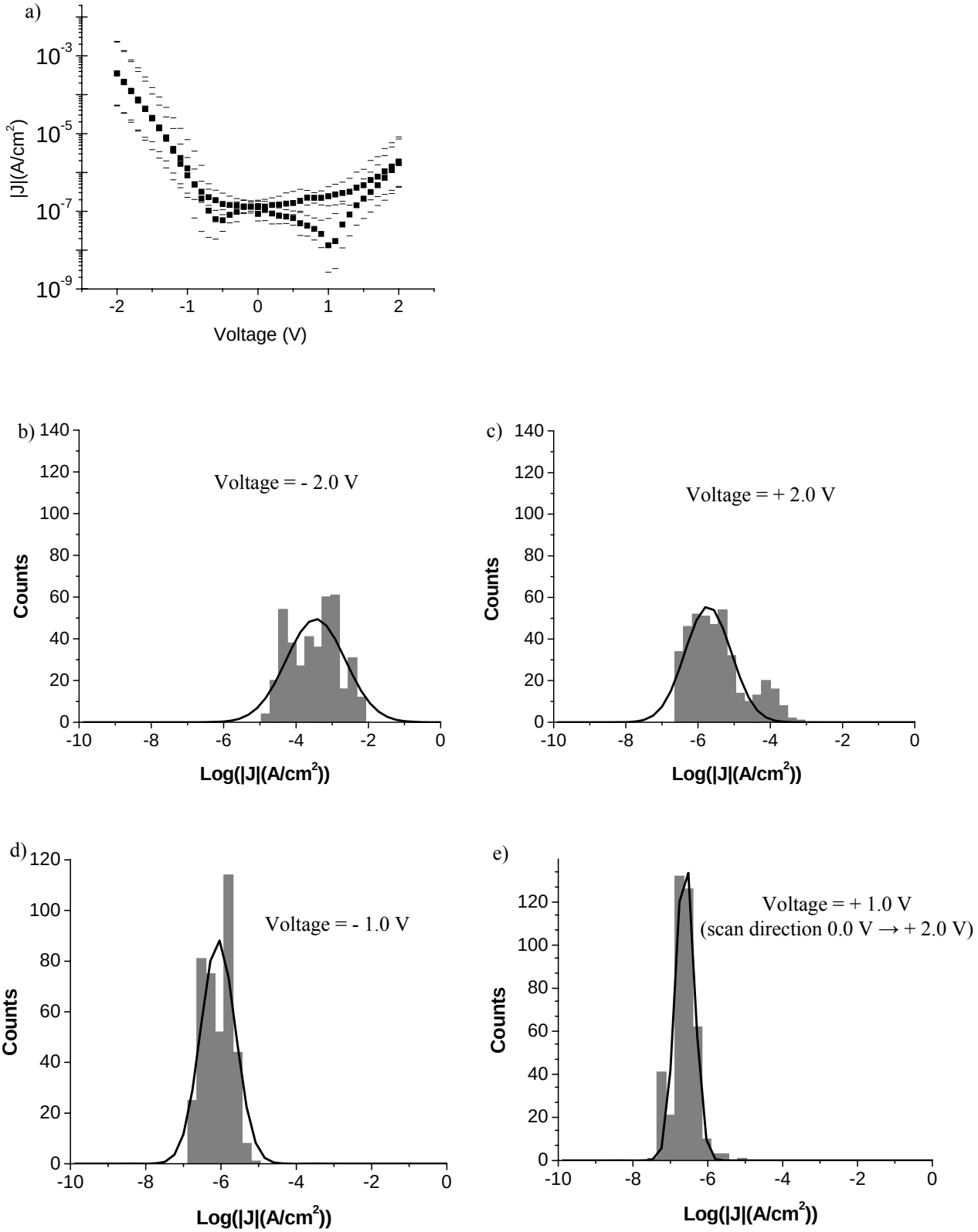

Figure S1: A semi-log plot of the averaged |*J*| vs *V* for junction Au^{TS}-βCDSAM/G1-PPI-$(BFc)_4$//(Ga_2O_3)EGaIn, ii (a), the statistical analysis for determining the averaged data point (log mean) at – 2.0 V (b), + 2.0 V (c), - 1.0 V (d), + 1.0 V (e). Shorts can not be seen on this scale as they have current densities of approximately $10^{\wedge 2}$.

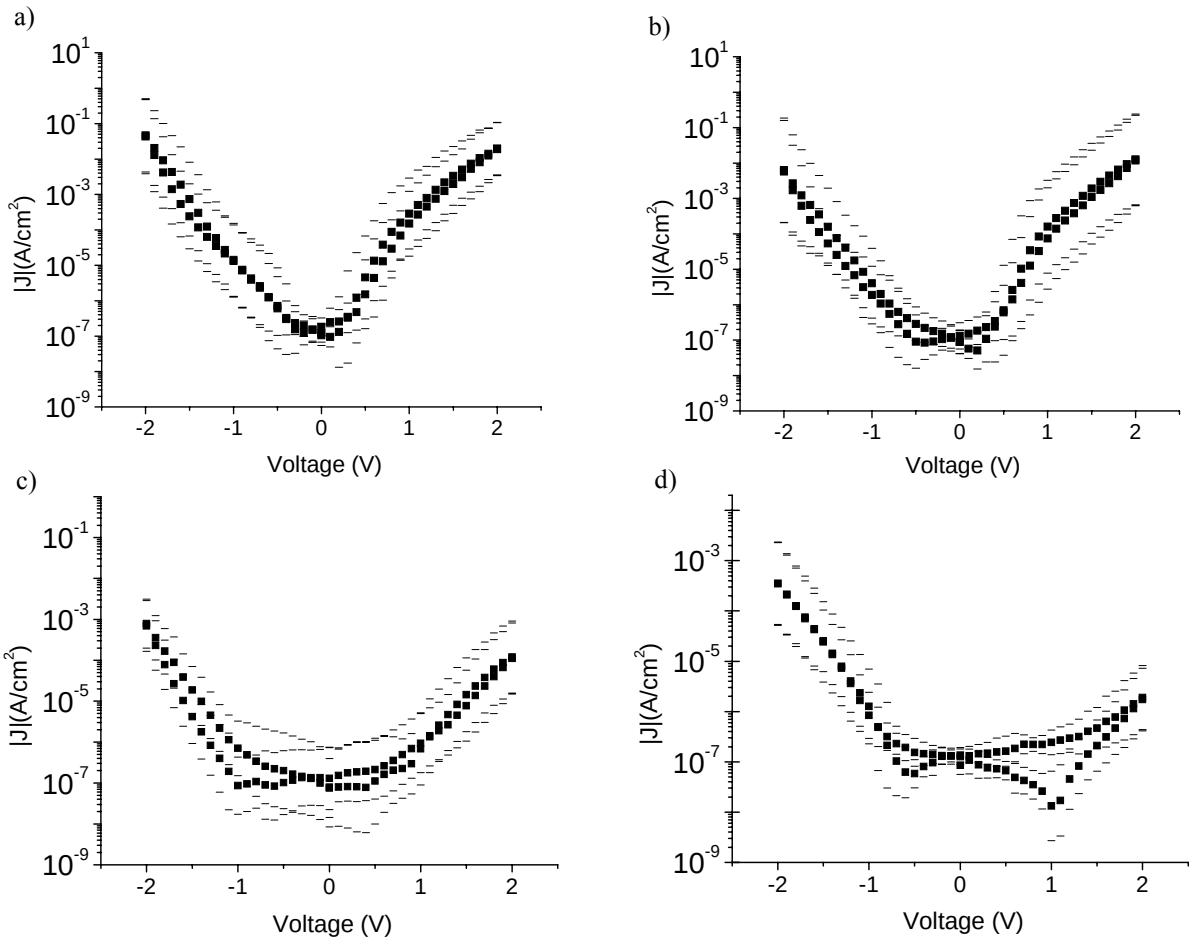

Figure S2: A semi-log plot of the averaged $|J|$ vs V for junction Au^{TS}-βCDSAM//(Ga_2O_3)EGaIn, iv (a), junction Au^{TS}-βCDSAM/G1-PPI-$(Ad)_4$//(Ga_2O_3)EGaIn, iii (b), junction Au^{TS}-βCDSAM/G1-PPI-$(Fc)_4$//(Ga_2O_3)EGaIn, i (c), junction Au^{TS}-βCDSAM/G1-PPI-$(BFc)_4$//(Ga_2O_3)EGaIn, ii (d).

Calculation of Rectification Ratio

The rectification ratio which is defined as $R = |J|(-2.0\ V)/|J|(+2.0\ V)$ was analyzed in the same fashion as the J measurements for each molecular junction and as previously published.[8] The R for each individual scan was calculated at ± 2.0 V for each supramolecular junction structure and plotted into histograms. Fitting the histograms with single Gaussian functions gave the log-mean value (average) R and the log standard deviation (with all errors stated representing one log-standard deviation, 68% of the distribution of the data is within one log-standard deviation of the log-mean, as shown in figure 3 in the manuscript).

Estimation of the HOMO Level Using Cyclic Voltammetry

The HOMO level for the G1-PPI-$(Fc)_4$ and G1-PPI-$(BFc)_4$ dendrimers were estimated as - 5.1 eV and - 5.0 eV respectively, relative to vacuum, from cyclic voltammetry using eq. 2, where $E_{NHE,abs}$ = absolute potential energy of the normal hydrogen electrode (- 4.5ev) and $E_{1/2\ NHE}$ = formal potential vs normal hydrogen electrode (which is 0.466eV).

$$E_{HOMO} = E_{NHE,abs} - eE_{1/2,NHE} \qquad (2)$$

Mechanism

We believe that a mechanism of charge transport applies to our junctions similar to that reported by Whitesides et al. for junctions of the form Ag^{TS}-$SC_{11}Fc$//(Ga_2O_3)EGaIn.[11] They also reported that tunneling (which is temperature independent) dominated the mechanism of charge transport at a positive bias and that hopping (which occurs when the HOMO level of the functional moiety overlaps with both the Fermi levels of the electrodes) dominated the mechanism of charge transport at a negative bias.

Shown in figure S3 is the molecular energy diagram for our supramolecular tunneling junction containing the βCD SAM + G1-PPI-$(BFc)_4$ dendrimer (junction ii) at a positive bias of 2.0 V (left) and a negative bias of 2.0 V (right). The dendrimers form a van der Waals contact with the (Ga_2O_3)EGaIn top-electrode, but are separated from the Au^{TS} bottom-electrode by the βCD SAM. The HOMO level of the BFc moiety is thus asymmetrically placed close to and coupled with the orbitals of the (Ga_2O_3)EGaIn top-electrode. The estimated HOMO level of the BFc dendrimers (from CV) is - 5.0 eV which lies very close to the Fermi levels of the electrodes, ~ - 5.0 eV for Au and ~ - 4.3 eV for (Ga_2O_3)EGaIn. Thus, the βCD SAM may have a similar function as the C_{11} alkyl chain in SAMs of $SC_{11}Fc$ and separates the Fc or BFc moieties from the bottom-electrode and, thus, provides asymmetry in the junctions, and the Fc and BFc moieties (regardless whether they interact or not with a CD moiety) of the dendrimers, as in the case of the SAMs of $SC_{11}Fc$, provide a HOMO level that is in energy slightly off set with the Fermi levels of the electrodes.

When performing our experiments, the (Ga_2O_3)EGaIn top-electrode was biased, and the Au^{TS} bottom-electrode was connected to ground. As most of the potential drops across the βCD SAM, the HOMO level of the BFc moiety follows the potential of the (Ga_2O_3)EGaIn top-electrode. At a positive bias the Fermi level of the (Ga_2O_3)EGaIn top-electrode decreases (- 6.3 eV) and therefore also does the HOMO level of the BFc (- 6.5 eV) (Figure S3 (left). The HOMO level of the BFc moiety does not change by the same amount as the Fermi level of the (Ga_2O_3)EGaIn top-electrode, because some of the applied potential will drop across the van der Waals interface. This leads to the BFc moiety not being able to participate in charge transport, as its HOMO level does not overlap with the Fermi levels of both electrodes, thus suggesting that tunneling is the dominant mechanism of charge transport at a positive bias. However at a negative bias the Fermi level of the (Ga_2O_3)EGaIn top-electrode increases (- 2.3 eV) (Figure S3 (left)) and therefore also does the HOMO level of the BFc (- 3.5 eV) (Figure S3 (right)). This leads to the BFc moiety being able to participate in charge transport, as its HOMO level does overlap with the Fermi levels of both electrodes, thus suggesting that hopping is a possible mechanism of charge transport at a negative bias. Therefore, the values of *J* are larger at a negative bias than at a positive bias and rectification occurs as the BFc moiety can only participate in charge transport at a negative bias.

All the details concerning potential drops, interface effects and position of HOMO levels relative to the electrodes, will be described in a separate paper.

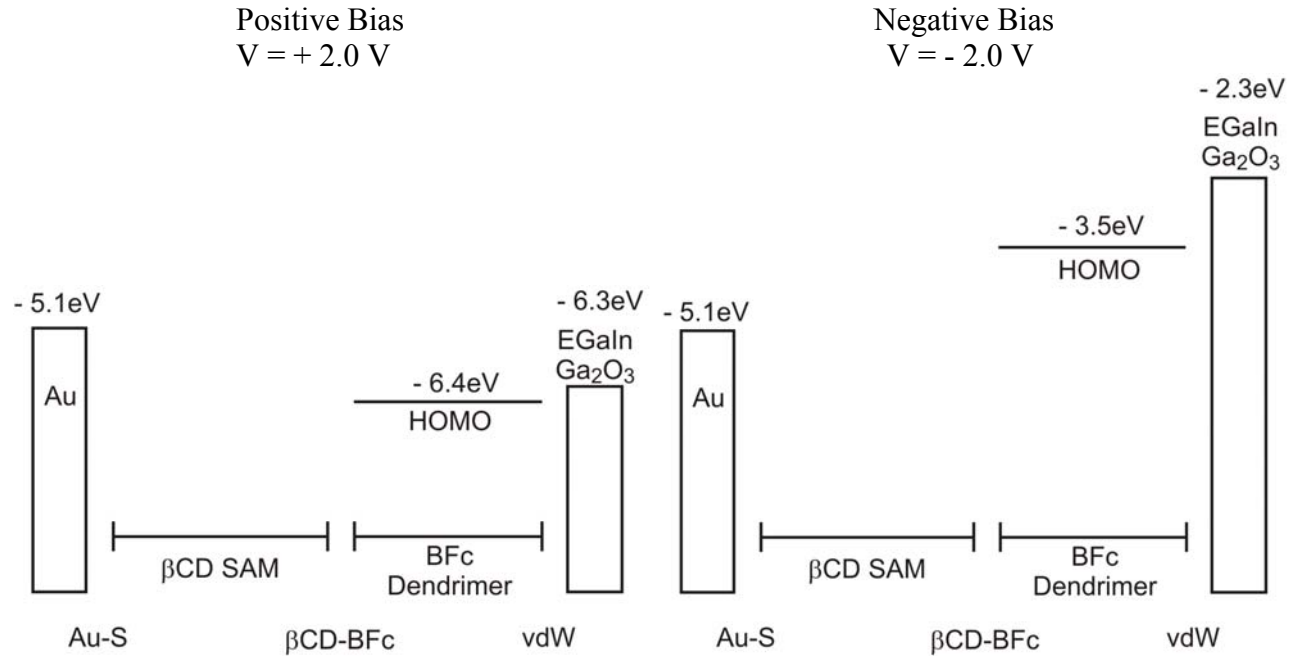

Figure S3: The proposed molecular energy diagram for Au^{TS}-βCDSAM/G1-PPI-$(BFc)_4$//(Ga_2O_3)EGaIn, (junction ii) at + 2.0 V (left) and - 2.0 V (right). Au-S = the gold-thiolate interface, βCD-BFc = the supramolecular host-guest interaction between the βCD SAM and the BFc terminal group of the dendrimer, vdW= van der Waals interface. Total thickness of the molecular layer = ~ 4.5nm, βCD SAM = ~ 2.5nm (calculated from EIS)[9] and G1-PPI-$(BFc)_4$ = ~ 2nm (estimated from molecular dynamic modeling).[10]

Current Density Variation

The difference in the average *J* of all the supramolecular junction structures does produce an unclear trend. The average values for junction iv are, as expected, higher than those observed for junctions i and ii. The values of the junctions iii and iv are, however, similar. We would expect the values of *J* for iii to be much lower than iv because junctions iii are thicker due to the presence of the monolayer of dendrimer which, in turn, would result in lower values of *J*. Table 1 shows that the Ad dendrimer forms a monolayer with a surface coverage of ~95%. Thus, also in these junctions the liquid metal top-contact may form direct contacts with the βCD SAM and increase the measured value of *J*. In addition, the log-standard deviations for these junctions are larger than for the other junctions which are probably the result of other variations between junctions that could affect *J*. In this article we are using rectification to investigate charge transport, which has the advantage of using, within the same tunneling junction, the current measured at the forward bias as the reference for the current measured at the reverse bias; eq. 1. This minimizes many of the uncertainties and complexities, such as contact resistances and contact areas, which are associated with comparing values of *J* obtained from different tunneling junctions. Even the most carefully prepared SAM-based tunneling junctions can exhibit larger variations in *J* (see histograms of *J*, Figure S 2b-e), but will not affect the value of *R*. Thus, despite the error in the values of *J*, the trend observed for the values of *R* holds.

References

[1] M. W. J. Beulen, J. Bugler, B. Lammerink, F. A. J. Geurts, E. M. E. F. Biemond, K. G. C. van Leerdam, F. C. J. M. van Veggel, J. F. J. Engbersen, D. N. Reinhoudt, *Langmuir* **1998**, *14*, 6424.

[2] M. Baars, A. J. Karlsson, V. Sorokin, B. F. W. de Waal, E. W. Meijer, *Angew. Chem. Int. Ed.* **2000**, *39*, 4262.

[3] I. Cuadrado, M. Moran, C. M. Casado, B. Alonso, F. Lobete, B. Garcia, M. Ibisate, J. Losada, *Organometallics* **1996**, *15*, 5278.

[4] C. A. Nijhuis, K. A. Dolatowska, B. J. Ravoo, J. Huskens, D. N. Reinhoudt, *Chem. Eur. J.* **2007**, *13*, 69.

[5] E. A. Weiss, G. K. Kaufman, J. K. Kriebel, Z. Li, R. Schalek, G. M. Whitesides, *Langmuir* **2007**, *23*, 9686.

[6] C. A. Nijhuis, F. Yu, W. Knoll, J. Huskens, D. N. Reinhoudt, *Langmuir* **2005**, *21*, 7866.

[7] R. C. Chiechi, E. A. Weiss, M. D. Dickey, G. M. Whitesides, *Angew. Chem. Int. Ed.* **2008**, *47*, 142.

[8] C. A. Nijhuis, W. F. Reus, G. M. Whitesides, *J. Am. Chem. Soc.* **2009**, *131*, 17814.

[9] M. W. J. Beulen, J. Bügler, M. R. de Jong, B. Lammerink, J. Huskens, H. Schönherr, G. J. Vancso, B. A. Boukamp, H. Wieder, A. Offenhäuser, W. Knol, F. C. J. M. van Veggel, D. N. Reinhoudt, *Chem. Eur. J.* **2000**, *6*, 1176.

[10] D. Thompson, *Langmuir* **2007**, *23*, 8441.

[11] C. A. Nijhuis, W. F. Reus, J. R. Barber, M. D. Dickey, G. M. Whitesides, *Nano Lett.* **2010,** 10, 3611